30 Mar 2001, 10:30 am - 12:30 pm

A Study on Failure Mechanism of Embankment Dams for Irrigation Damaged by the 1995 Hyogoken-Nanbu Earthquake

Kazunori Uchida
Kobe University, Japan

Tuyosi Torii
Construction Project Consultants, Japan

Syuichi Tsujino
Satou-Kogyo Corp. Ltd., Japan

Susumu Ando
Kajima Corp. Ltd., Japan

Keiji Higasio
Kajima Corp. Ltd., Japan

Author
Kazunori Uchida, Tuyosi Torii, Syuichi Tsujino, Susumu Ando, Keiji Higasio, and Taniaki Yamamoto

A STUDY ON FAILURE MECHANISM OF EMBANKMENT DAMS FOR IRRIGATION DAMAGED BY THE 1995 HYOGOKEN-NANBU EARTHQUAKE

Kazunori Uchida
Kobe University
Nada-ku, Kobe-JAPAN-657-8501

Tuyosi Torii
Construction Project Consultants
Nishi-ku, Osaka-JAPAN-550-0004

Syuichi Tsujino
Satou-Kogyo Corp. Ltd
Tokyo-JAPAN-103-8639

Susumu Ando
Kajima Corp. Ltd
Nishi-ku, Osaka-JAPAN-550-0011

Keiji Higasio
Kajima Corp. Ltd
Nishi-ku, Osaka-JAPAN-550-0011

Taniaki Yamamoto
Hyogo Prefecture Office
Chuo-ku, Kobe-JAPAN-650-8567

ABSTRACT

The objects of this investigation are to examine the following mechanism of embankment dams for irrigation damaged by the 1995 Hyogoken-Nanbu Earthquake; 1) the mechanism and process of collapse for the Idenoshiri-Ike embankment dam using the effective stress earthquake response analysis; 2) the mechanism of upper slope failure for the Sugatadani-Ike embankment dam using the total stress earthquake response analysis as well as the slope stability analysis with seismic intensity. As a result, the following conclusions are obtained for each objects; 1) the mechanism and process of collapse due to liquefaction can be analyzed that the liquefied areas initially occurred at the toes of upper and lower slopes are extended and connected to make flow downward the volume of embankment and that the result of this analysis is consistent with the real damaged situation; 2) the mechanism of upstream slope failure can be explained only with considering the increase of excess pore pressure in the upstream slope, not extending complete liquefaction, using the both analyses.

INTRODUCTION

In Hyogo Prefecture, there were about 51,000 embankment dams for irrigation, especially in Awaji Island, about 24,000 ones are located. Due to the strong ground motion of the 1995 Hyogoken-Nanbu Earthquake, many embankment dams were suffered severe damage such as sliding failure of upstream slope, longitudinal cracks occurred on dam crest and slope, etc. Fortunately, only two embankment dams, Idenoshiri-Ike and Niteko-Ike, were catastrophically failed, and no secondary disaster was occurred. *Figure 1* shows a relationship between the closest distance from the fault line and the number of damaged embankment dams for irrigation in Awaji Island and Honshu Island. About 950 embankment dams were damaged in Awaji Island as they were very close to the epicenter of the earthquake. *Fig.1* shows that all of these damaged dams were distributed within 10 km from the fault line. The Idenoshiri-Ike dam located in the northwest part of this island was suffered a catastrophic failure of the central part of the dam due to soil liquefaction. This cause of failure was estimated by observing many sand boils on the reservoir bed. On the other hand, *Fig.1* shows that many damaged embankment dams were distributed over 10 to 25 km distance from the fault line in Honshu Island. The Sugatadani-Ike dam was located in the southeast of Ono City in Hyogo Prefecture, about 26 km far from the fault line. This dam was suffered a sliding damage of the whole upstream slope. It is noted that there were many embankment dams suffered the same damage as the Sugatadani-Ike one, but no dams suffered sliding damage of downstream slope.

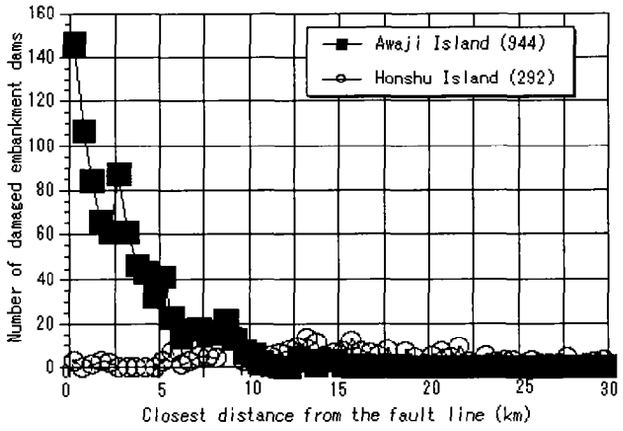

Fig. 1. Relationship between the closest distance from the fault line and the number of damaged embankment dams

In this paper, the failure mechanism of the two embankment dams mentioned above were examined by different analyses; the Idenoshiri-Ike dam was analyzed with an effective stress earthquake response analysis; the Sugatadani-Ike dam with a total stress earthquake response analysis as well as a slope stability analysis with horizontal seismic coefficient.

LIQUEFACTION FAILURE MECHANISM OF THE IDENOSHIRI-IKE EMBANKMENT DAM

The mechanism and process of the collapse of Idenoshiri-Ike embankment dam by soil liquefaction during the 1995 Hyogoken-Nanbu Earthquake was examined by an effective stress analysis. The Idenoshiri-Ike dam is located in the northwestern part of Awaji Island. It was a homogeneous type earth-fill dam with *155m* long, *5.5m* high, and *17,500m*^{3} storage capacity of reservoir. At the time of the earthquake, the ceter part of dam collapsed completely; many cracks in the longitudinal direction appeared as showing in *Fig.2*. A cross-section of collapsed embankment and *SPT N*-value are also shown in *Fig.2* [The Department of Agriculture, 1996]. Soil liquefaction of the foundation ground was supposed to be the cause of the failure because many sand boils were observed on the reservoir bed and at the downstream paddy field.

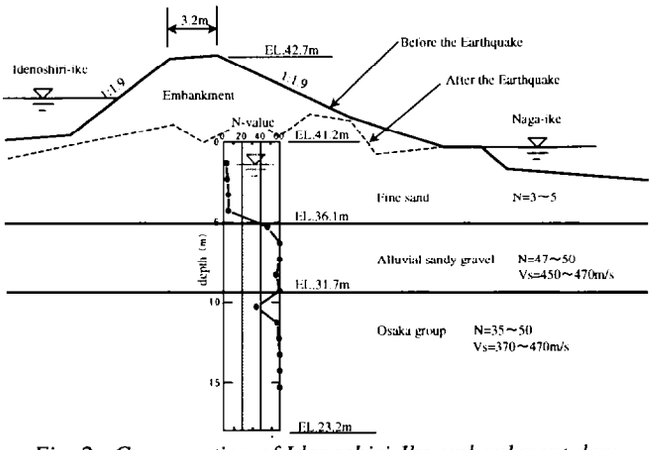

Fig. 2. Cross section of Idenoshiri-Ike embankment dam

Analytical Procedure

The effective stress analysis code for two-dimensional problems, *TARA-3* [Finn et al, 1986], was employed. A hyperbolic model was used for shear stress-shear strain relationships and declinations of shear modulus and shear strength with decreasing effective stress was taken into account. Development of excess pore water pressure was computed by the two parameters model, which was modified from Martin-Finn-Seed model [Martin et al, 1978]. The FEM model is shown in *Fig.3*. Since no acceleration record was obtained in Awaji Island, the record obtained at Kobe University during the 1995 Hyogoken-Nanbu Earthquake was used as an input motion. A maximum acceleration was adjusted to be *441Gal (0.45g)* based on the maximum accelerations evaluated from the falling down of tombstone tumbles. An input acceleration time history is shown in *Fig.4*.

The model parameters for the analysis are shown in *Table 1*. The liquefaction parameters for the two parameters model were decided by simulating the liquefaction strength obtained by cyclic triaxial tests of undisturbed samples. A comparison between the test and the simulation is shown in *Fig.5*; and these are agreed very well. No test data was available for the alluvial

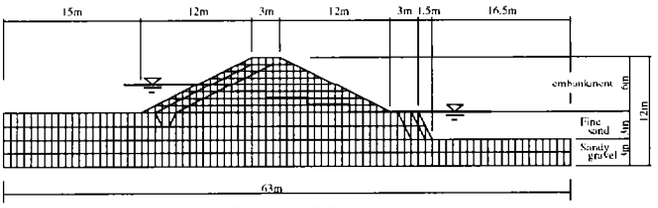

Fig. 3. FEM model

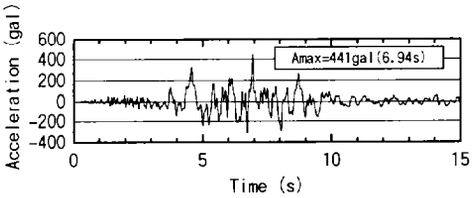

Fig. 4. Input motion

Table 1 Model parameters

Layer	Embankment and Fine sand	Alluvial sandy gravel
Strength	ϕ =30° c=0.0 kN/m^2	ϕ =40° c=0.0 kN/m^2
Shear modulus	Go=60000 kN/m^2 (σ_{v0}'=55 kN/m^2)	Go=450000 kN/m^2 (σ_{v0}'=100 kN/m^2)

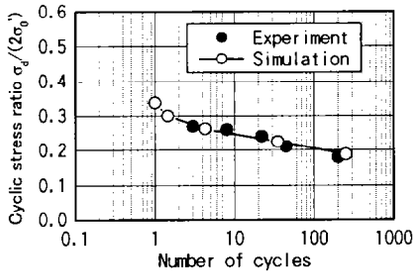

Fig. 5. Liquefaction strength

sandy gravel layer, development of excess pore water pressure in this layer was not considered because *SPT N*-value is very large to be more than *47* as seen in *Fig.2*.

Discussion

Liquefied areas are shown in *Fig.6*. Time histories for response acceleration are shown in *Fig.7*, and ones for excess pore water pressure in *Fig.8*. Judging from analyzed displacement, the whole embankment moves toward the downstream side. From these results obtained by the analysis, the process of the collapse of this embankment dam is estimated as follow;

a) Until about *3.5* seconds passing from the beginning of the earthquake, amplification of acceleration from the bottom to the crest is about two times as shown in *Fig.7* and the liquefaction doesn't occur in all elements (as seen in *Fig.6*).

b) During *3.5-4.0* seconds, the element *E1* (see *Fig.8*) near the upstream slope is liquefied, then elements in the downstream side are liquefied. The liquefaction area expands in nearby areas in the subsequent large pulse at about *4.5* seconds.

c) Liquefied area expands to the center part until *7* seconds when input acceleration shows peak values. At *7* seconds, liquefaction area form upstream to downstream sides jointed,

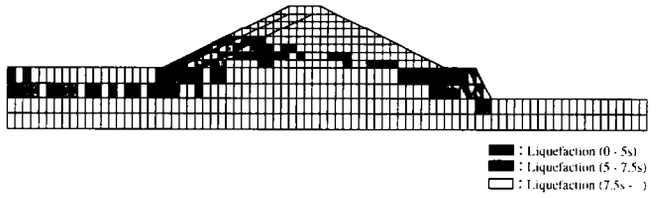

Fig. 6. Liquefied zone during shaking

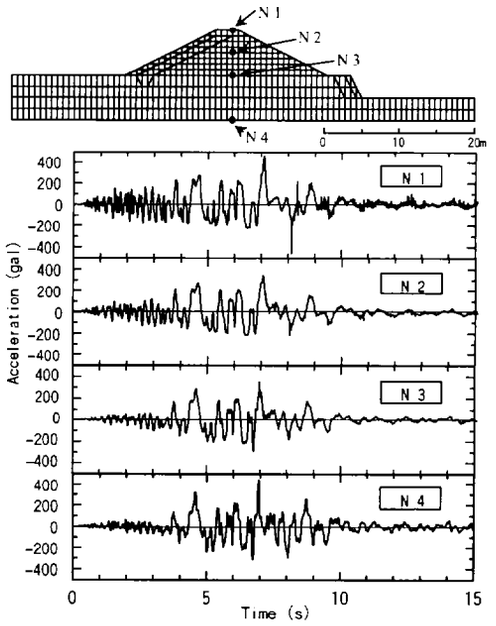

Fig. 7. Acceleration time history

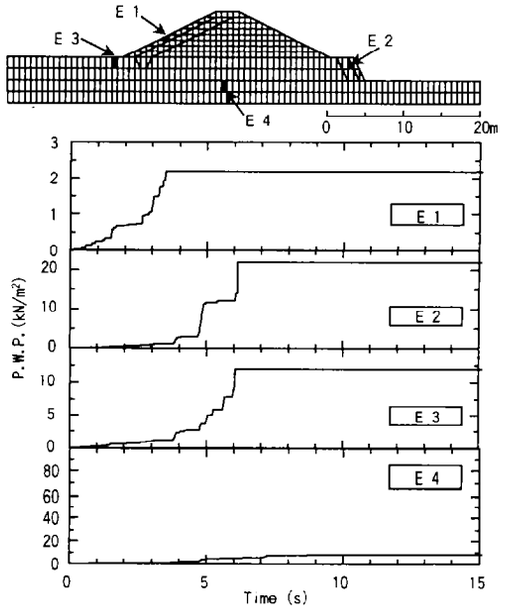

Fig. 8. Pore water pressure time history

resulting in very week layer of the bottom of the embankment dam.

The failure of the embankment dam is supposed to be caused by the formulation of this week layer (liquefied layer).

SLIDING FAILURE MECHANISM OF THE SUGATADANI-IKE EMBANKMENT DAM

The failure mechanism of the Sugatadani-Ike embankment dam damaged by the 1995 Hyogoken-Nanbu Earthquake was examined by slope stability analysis based on the static seismic coefficient method and earthquake response analysis. These analyses were carried out using characteristic values obtained from surveys such as boring tests conducted after the earthquake. The results evaluated from such analyses are in good agreement with the actual damage, and the conditions caused the failure of this embankment are clarified.

Overview of Damage

The Sugatadani-Ike embankment dam is located on a hill with elevations of about *90m* in the southeast area of Ono City in Hyogo Prefecture. It was a homogeneous type earth-fill dam with *98m* long and *12m* high. *Fig.9* shows an overview of the cross section of this damaged embankment. The water level of reservoir during the earthquake was about half of the design high water level, and the upstream slope was damaged by the slide along the whole length of the embankment dam with gaps of about *4m* at the crest.

Since the closest distance from the fault line to this embankment dam was estimated to be *26.4km*, from the relationship between the horizontal acceleration and the closet distance from the fault line in the region [Toki et al, 1995], the maximum acceleration at the site is estimated to be approximately *200Gal (0.20g)* (*160Gal (0.16g)* for stiff ground and *230Gal (0.23g)* for soft ground). It is considered that liquefaction was not caused due to the earthquake because of the acceleration was relatively small and no sand boils were observed near the reservoir.

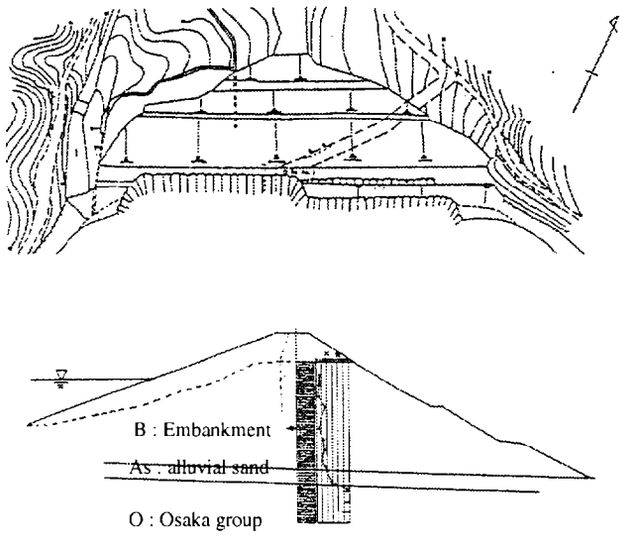

Fig. 9. Damage of the Sugatadani-Ike embankment dam [The Department of Agriculture, 1996]

Determination of Characteristics Values

Several tests such as laboratory soil test, boring test, *PS* logging, in-situ soil density test, and in-situ permeability test were conducted after the earthquake in order to obtain the characteristic values of the foundation stratum and the embankment. The soil profile of the embankment and the foundation stratum are shown in *Table 2*. The embankment consisted of sandy soil with *N*-values ranging from 4 to 17. The calculation and analysis were carried out using the cross section at the center of the embankment. The soil properties used for the earthquake response analysis and the static seismic coefficient method are shown in *Table 3* and *Fig.10*. The strength parameter of the embankment was estimated from the triaxial compression tests, and that of the foundation stratum was estimated from the *N*-values. The initial shear modulus G_0 was determined based on *Vs* from *PS* logging, and the strain-dependency with respect to the shear modulus and the damping ratio was estimated based on the existing literatures.

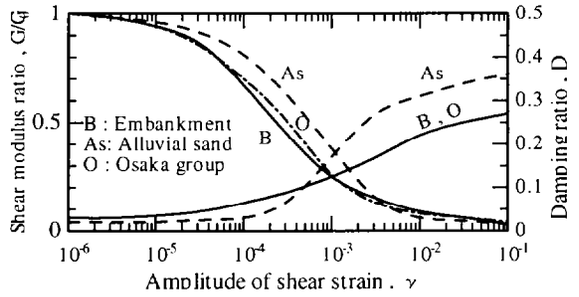

Fig. 10. Strain-dependency of embankment and foundation

Evaluation by the Static Seismic Coefficient Method

Estimation method for excess pore water pressure. *Fig.11* shows the relationship between pore water pressure ratio *Lu* and liquefaction resistance factor F_L used for analysis. The liquefaction resistance factor F_L was calculated from the specifications on the literature (see Fig.11).

Table 2 Soil profile of the dam and the foundation stratum

Ground stratum	Soil type	N-value
Embankment	Sandy gravel with clay. Gravel is mainly 0.3～1.5cm round gravel. Under the embankment contains a lot of gravels. Ip(Plasticity Index)=13, F.C.=30%	4～17
Alluvial sand layer	Less fine grained coarse sand include gravel.	20
Foundation ground	Sandy gravel with clay. Gravel is mainly 0.3～1.5cm round gravel. Matrix is hardened sand with clay.	More than 50

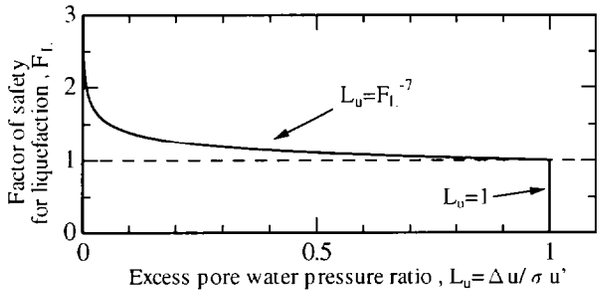

Fig. 11. Relationship between Lu and F_L [Public Works Research Institute, 1997]

Equation for calculating safety factor. Safety factor *Fs* was calculated using in the Design Specification for Dams (revision) by incorporating the effect of excess pore water pressure [Japan Commission on Large Dams, 1978],

$$Fs = \frac{\Sigma (c\,l + (N-U-Ne-Ue)\tan\phi)}{\Sigma (T+Te)} \qquad (1)$$

where, in each slice used for the stability analysis, c, ϕ: strength parameters for the slip surface, l: slip surface length of the slice, N,T: vertical and tangential component of the load acting on the slip surface, Ne,Te: vertical and tangential components of the seismic load acting on the slip surface, U: pore water pressure-induced load acting on the slip surface, Ue: excessive pore water pressure-induced load acting on the slip surface ($= \Delta u\, l$, Δu: excess pore water pressure).

Table 3 Soil properties used in analysis [Tateishi, 1996]

Item	Embankment				Soft clay (Bed layer of the reservoir)	Alluvial sand layer	Sandy gravel (Osaka group layer)
	0～3m*	3～6m*	6～9m*	9m～*			
ρ_t t/m³	1.73(partially saturated) , 1.94(saturated)				1.94	2.06	2.18
C kN/m²	29.4	9.81			4.9	0	49
ϕ °	26.5				0.0	36	40
Permeability k cm/sec	5×10^{-5}				5×10^{-5}	1×10^{-3}	
SPT N-value	5	5	11	13	0	20	50
Optimized *N*-value	14	10	17	17	—	—	—
R_L**	0.21	0.21	0.28	0.28	—	0.28	0.5
Shear Velosity *Vs* m/sec	100	100	170	190	100	260	320
Go MN/m²	18.5	21	59	74	18.5	140	230
Poisson's Ratio ν	0.35(partially saturated) , 0.45(saturated)				0.45	0.45	
D	0.05				0.05	0.035	

* Depth is the distance from the ground surface

** R_L : Cyclic triaxial strength ratio [Japan Road Association, 1996]

*** D : initial damping ratio

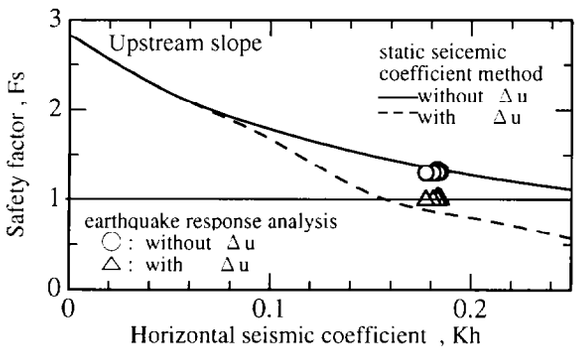

(a) upstream slope

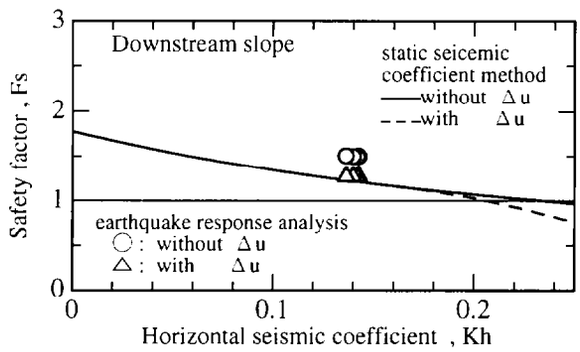

(b) downstream slope

Fig. 12. Relationship between safety factor and horizontal seismic coefficient

Relationship between horizontal seismic coefficient and safety factor. The solid lines in *Fig. 12* show the relationship between safety factor *Fs*, which was obtained from equation (1) by assuming *Ue=0*, and horizontal seismic coefficient *Kh*. The calculations are conducted with only a circular arc given the minimum safety factor where *Kh=0.1*. The shape of seepage surface was calculated by saturated and unsaturated seepage analysis. As shown in *Fig. 12*, the safety factor of the downstream slope is smaller than that of the upstream slope, with the limit horizontal seismic coefficient *Khc* (horizontal seismic coefficient for *Fs=1.0*) for the upstream slope being *0.29*, and *Khc* for the downstream slope being *0.23*. Considering that the maximum ground acceleration at the site was approximately *200Gal(0.2g)*, the upstream slope of this reservoir theoretically should not collapse if the horizontal seismic coefficient is about *0.2*. In addition, the lower safety factor for the downstream slope contradicts the fact that the failure occurred only on the upstream slope. Records of this earthquake also show that there were several cases where the upstream slope of the embankment or the whole embankment collapsed, but no case where only downstream slope collapsed. This indicates that the above calculation based on the static seismic coefficient method cannot explain the actual damage, where only the upstream slope collapsed. The possible reason for this is that the effect of excess pore water pressure was not taken into consideration in the above calculation.

The dot lines in *Fig.12* show the relationship between *Fs*, for which the effect of excess pore water pressure Δu obtained from *Fig.11* is taken into account, and *Kh*. In this figure, the effect of Δu is observed, where *Kh* is equal to or larger than *0.1* for the upstream slope, and equal to or larger than *0.2* for the downstream slope. *Khc* is *0.15* and *0.2* for the upstream slope and downstream slope, respectively. Therefore it can be concluded that the cases where only the upstream slope collapses can be explained by static seismic coefficient method if the effect of pore water pressure is taken into account.

Evaluation by the Earthquake Response Analysis

Total stress earthquake response analysis. The earthquake response analysis was carried out based on the equivalent linear method (*FLUSH*). The main-shock record (*EW* component) of the earthquake observed at the Kobe University was used for the input ground motion at the site with modifying to have a maximum acceleration of *200Gal(0.2g)*. In the mesh model used for finite element method analysis, the left and right ends are set to be the energy-transmitting boundary, and the bottom end (foundation stratum) to be the viscous boundary.

The safety factor for the total stress analysis was calculated using shear and normal stresses acting on the slip surface, which can be determined by the composite stress of dynamic and static stresses (the stress obtained from static FEM analysis where the self-weight and buoyancy acting on the embankment). The symbol ○ in *Fig.12* shows the relationship between *Fs* at, before, and after such a time that the safety factor becomes minimum, and the horizontal seismic coefficient which is equivalent to the average horizontal inertia force acting on the slip mass, *Khe*. For the upstream slope, the *Fs-Kh* relationship obtained from the earthquake response analysis is in good agreement with that obtained from the static seismic coefficient method. For the downstream slope, however, the *Fs-Kh* relationship by the earthquake response analysis falls above the curve obtained from the static seismic coefficient method. Judging from the maximum value for *Khe* shown in *Fig.12*, the actual maximum horizontal seismic coefficient is expected to have been approximately *0.18*. This roughly agrees with the equivalent value of the coefficient calculated from the maximum ground motion acceleration (*=200Gal(0.2g)*). It should be noted, however, that where the horizontal seismic coefficient is about *0.18*, *Fs* is calculated to be about *1.3* and this does not agree with the actual condition of failure.

Effective stress response analysis. The effective stress response analysis (*TARA-3*) was carried out to verify the mechanism of upstream slope failure. *Fig.13* shows the distribution of excess pore water pressure obtained from this analysis. This figure indicates that excessive pore water pressure tends to develop near the upstream slope. It can also be seen from this figure that the location where the excess pore water pressure ratio develops close to *0.9* is limited to a small area near the surface of the upstream slope, so liquefaction of the whole embankment does not occur. The symbol △ in *Fig.12* shows *Fs*, for which the effect of excess pore water pressure obtained from the effective

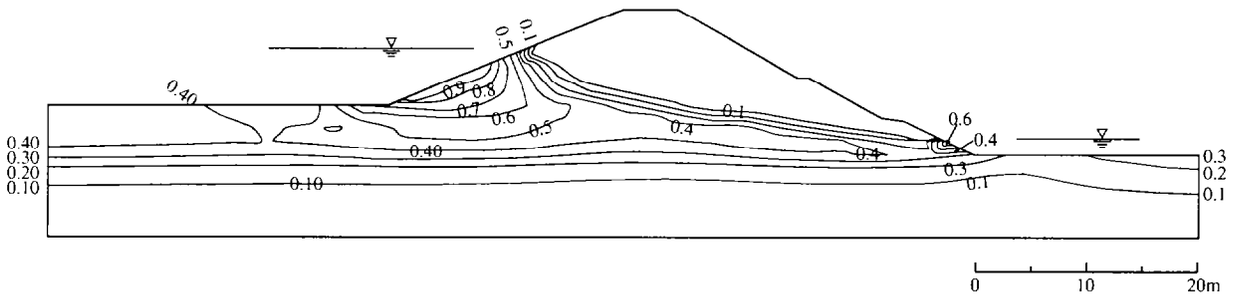

Fig. 13. Distribution of excess pore water pressure ratio $\Delta u / \sigma_m'$ obtained from the effective stress response analysis (Δu : excess pore water pressure, σ_m' : mean principal stress)

stress analysis was incorporated into the results of the total stress response analysis. When the effect of excess pore water pressure is considered, *Fs* is calculated to be approximately *1.0* for the upstream slope and more than *1.0* for the downstream slope, which is in agreement with the actual case where only the upstream slope collapses.

As described above, it was found that the embankment damage where only the upstream slope collapsed could not be explained without the development of excess pore water pressure in the upstream slope of embankment during the earthquake. It is therefore concluded that the collapses of embankment caused by the increase of pore water pressure as well as the low shear strength of the embankment materials.

CONCLUSIONS

In this paper, the mechanism of the collapse for the two embankment dams for irrigation, Idenoshiri-Ike and Sugatadani-Ike, were analytically examined. For the former, the effective stress earthquake response analysis was used, and for the latter, the slope stability analysis using the static seismic coefficient method and earthquake response analysis. As a result, the following conclusions are obtained.

1) The mechanism and process of collapse due to soil liquefaction can be analyzed that the liquefied areas initially occurred at the toes of upper and lower slopes are extended and connected to make flow downward the volume of embankment. The result of this analysis is consistent with the real damaged situation.
2) The mechanism of upstream slope failure can be explained only with considering the increase of excess pore pressure in the upstream slope, not extending complete liquefaction, using the both analyses.

This investigation was conducted as a part of the activities of the Sub-Committee 2 for Soil and Foundation in the Research Committee on the Damage by the 1995 Hyogoken-Nanbu Earthquake, the Kansai Branch of the Japan Society of Civil Engineers.

REFERENCES

Finn, W. D. L., Yogendrakumar, M., Yoshida, N. and Yoshida, H. [1986]. TARA-3, a program for nonlinear static and dynamic effective stress analysis, Soil Dynamic Group, University of British Columbia, Vancouver.

Japan Commission on Large Dams [1978]. Design specification for dams, 2nd revision, (in Japanese).

Japan Road Association [1996] Specification for highway bridges, Part-V, Seismic Design, (in Japanese).

Martin, G. R., Finn, W. D. L., and Seed, H. B. [1975]. Fundamentals of liquefaction under cyclic loading, FED, ASCE, Vol. 101, No. GT5, pp. 423-438.

Public Works Research Institute [1997]. Design and construction manual of sand improvement method against liquefaction of levee, Ministry of Construction, Record of Public Works Research Institute No.3513, (in Japanese).

Tateishi, T. [1996]. In-situ tests and laboratory tests results of embankment dams for irrigation failed by the 1995 Hyougoken-Nanbu Earthquake, Committee back data, Committee of the Damage by the 1995 Hyogoken-Nanbu Earthquake, the Kansai Branch of the Japan Society of Civil Engineers, (in Japanese).

The Department of Agriculture, Forestry and Fisheries, Hyogo Prefecture [1996]. The report of earthquake damage for agriculture due to the 1995 Hyogoken-Nanbu Earthquake, (in Japanese).

Toki, K., Goto, Y., Ejiri, J. and Sawada, S. [1995]. A brief review of source effects and local site effects during the 1995 Hyogoken-Nanbu Earthquake, Journal of the Japan Society of Civil Engineers, Vol.80, No.9, pp.32-43, (in Japanese).